Research Square

Preprints are preliminary reports that have not undergone peer review.
They should not be considered conclusive, used to inform clinical practice,
or referenced by the media as validated information.

Choroidal thickness in the macula, nasal midperiphery, and temporal midperiphery in schoolchildren

Takahiro Hiraoka
thiraoka@md.tsukuba.ac.jp
University of Tsukuba
Masato Tamura
Topcon Corporation
Yoshikiyo Moriguchi
Topcon Corporation
Riku Kuji
Topcon Corporation
Toshihiro Mino
Topcon Corporation
Masahiro Akiba
Topcon Corporation
Yosuke Takahashi
Yoshino Eye Clinic
Kenichi Yoshino
Yoshino Eye Clinic
Asaki Suzaki
Menicon Co., Ltd
Keiji Sugimoto
Menicon Co., Ltd
Tetsuro Oshika
University of Tsukuba

Article

Keywords: choroidal thickness, axial length, myopia, midperiphery, schoolchildren, asymmetry

Posted Date: May 13th, 2026

DOI: https://doi.org/10.21203/rs.3.rs-6875224/v1

License: This work is licensed under a Creative Commons Attribution 4.0 International License.
Read Full License

Additional Declarations: No competing interests reported.

Abstract

This study aimed to quantitatively evaluate choroidal thickness (ChT) in the macula, nasal midperiphery, and temporal midperiphery in schoolchildren and to investigate its associations with axial length (AL) and spherical equivalent refractive error (SE). A total of 174 eyes from 87 children (mean age: 9.82 ± 2.42 years) were examined using high-speed swept-source optical coherence tomography (SS-OCT). ChT was measured over a 3-mm transverse section centered at the macula and at 39° nasal and temporal eccentricities. After correcting image distortion, ChT was calculated as the perpendicular distance from Bruch's membrane to the choroid-sclera interface. Mean ChT values were 266.3 μm in the macula, 194.4 μm nasally, and 158.7 μm temporally, showing significant regional differences ($P < 0.0001$). ChT was negatively correlated with AL and positively correlated with SE in the macular and temporal regions, but not in the nasal region. When compared to adults, schoolchildren exhibited significantly thicker temporal ChT, suggesting that temporal choroidal thinning may occur with age and axial elongation. These findings indicate a nasal-temporal asymmetry in peripheral ChT during childhood and highlight the potential of temporal ChT as a biomarker for early ocular growth related to myopia. Longitudinal studies are warranted to establish causality.

Introduction

The digitalization of society has rapidly accelerated, with mobile devices such as smartphones and tablets now deeply embedded in our daily lives as indispensable tools. Screen time continues to rise, transforming our visual environment at an unprecedented pace. Amid these changes, the sharp increase in the number of individuals with myopia has emerged as a global issue. Projections suggest that by 2050, approximately 50% of the global population will be myopic, with high myopia affecting around 10% (940 million people)[1]. This surge raises significant concerns about the rising prevalence of blindness caused by myopia-related eye diseases, including myopic maculopathy, glaucoma, and retinal detachment[2]. The economic repercussions are equally substantial, with the global productivity loss attributed to myopia estimated at approximately $260 billion USD annually[3].

In response to this alarming trend, the urgent need for proactive interventions has gained worldwide recognition, prompting the clinical application of various myopia control strategies[4]. Although the exact mechanisms underlying myopia control remain unclear, choroidal changes have increasingly been implicated in the efficacy of several interventions, such as orthokeratology[5–9], atropine eye drops[10–12], multifocal contact lenses[13–15], specially designed spectacles[16–17], and red-light therapy[18–22].

Compensatory changes in choroidal thickness (ChT) in response to optical defocus were first observed in experimental chick models[23]. Specifically, the choroid was found to adjust its thickness to compensate for refractive errors: positive lenses that induce myopic defocus (focusing in front of the retina) cause the choroid to thicken, whereas negative lenses that induce hyperopic defocus (focusing behind the retina) result in choroidal thinning[24]. These compensatory changes have also been confirmed in humans, highlighting that the choroid is a dynamic structure responsive to visual stimuli[25–27].

Additionally, studies in both animals and humans have shown that axial length increases during accommodation[28–31], indicating that frequent or prolonged accommodation may contribute to irreversible axial elongation. The choroid plays a crucial role in regulating eye growth and scleral remodeling by modulating the release and diffusion of growth factors[32]. According to Troilo et al.[33], during the early stages of myopia development, the choroid may act as a barrier to limit the diffusion of growth factors or serve as a mechanical buffer to resist scleral stretching, thereby restricting axial elongation and slowing the progression of myopia.

Ocular development varies between individuals, with different growth patterns proposed, including uniform expansion of the entire eyeball, equatorial extension, and posterior pole elongation[34]. Among these, equatorial extension—unlike posterior pole elongation, which is primarily associated with scleral fragility in pathological myopia[35]—is considered the dominant growth pattern in schoolchildren with myopia. Evidence supporting equatorial extension includes the frequent occurrence of lattice degeneration in the peripheral retina, even in cases of mild myopia, particularly around the equatorial region[36]. This suggests that the equatorial area is the primary site of ocular changes during the development of school-age myopia, emphasizing the importance of investigating morphological changes in the peripheral regions rather than focusing solely on the posterior pole. However, previous imaging techniques had limitations in obtaining accurate biometric measurements of the peripheral area, leaving this important aspect of ocular development unresolved.

Recent advancements in OCT technology have made it possible to evaluate ChT in the midperipheral regions[37–39]. Studies in adults have reported ChT measurements in areas centered 39° nasally and temporally from the fovea using high-speed swept-source optical coherence tomography (SS-OCT) [40]. In this study, we assessed midperipheral ChT in schoolchildren using the same imaging device and examined its associations with refraction and axial length (AL). Additionally, we compared our findings with previously reported data from adult studies to identify potential differences in choroidal characteristics between age groups.

Results

A total of 174 eyes from 87 participants (43 boys and 44 girls) were included in this study. The participants' ages ranged from 6 to 15 years, with a mean age of 9.82 ± 2.42 years. The SE ranged from − 6.88 to 3.25 D, with a mean of − 1.25 ± 1.84 D. The cylindrical refractive error ranged from − 3.00 to 0.00 D, with a mean of − 0.65 ± 0.55 D. The AL ranged from 21.47 to 26.92 mm, with a mean of 23.77 ± 1.16 mm. Eyes with staphyloma were not included in the study.

ChT

The ChT measurements for each region were as follows: 266.3 ± 63.2 μm (range: 129.7 to 417.6 μm) in the macular region, 194.4 ± 39.5 μm (range: 85.6 to 305.0 μm) in the nasal midperiphery, and 158.7 ± 41.4 μm (range: 58.6 to 264.0 μm) in the temporal midperiphery. Significant differences in ChT were

observed among the three regions (P < 0.0001, one-way ANOVA), with the macular region showing the greatest ChT, followed by the nasal midperiphery and the temporal midperiphery (P < 0.0001 for all pairwise comparisons, Bonferroni correction) (Fig. 3).

Correlation Analysis

Scatter plots of ChT versus AL revealed significant correlations in the macular region (P < 0.0001, R = − 0.465, Pearson correlation test) and the temporal midperiphery region (P = 0.016, R = − 0.182), but no significant correlation in the nasal midperiphery region (P = 0.059, R = 0.143) (Fig. 4). Similarly, significant correlations between ChT and SE were observed in the macular region (P < 0.0001, R = 0.368) and the temporal midperiphery region (P < 0.001, R = 0.313), whereas no significant correlation was found in the nasal midperiphery region (P = 0.846, R = − 0.015).

Comparison of ChT between schoolchildren and adults

The ChT measurements for schoolchildren in this study were compared to those for adults from our previous research[40]. No significant differences were observed between schoolchildren and adults in the macular and nasal regions (P = 0.943 and P = 0.313, respectively; unpaired t-test). However, a significant difference was found in the temporal region (P < 0.0001) (Fig. 5).

Discussion

This study is the first to quantitatively evaluate ChT in the midperipheral fundus in a large cohort of schoolchildren. The findings demonstrated that ChT in the midperiphery (194.4 μm in the nasal region and 158.7 μm in the temporal region) is significantly thinner than in the macular region (266.3 μm). Moreover, the ChT in the temporal region was significantly thinner than in the nasal region. Regarding macular ChT, a study with a similar design to ours was previously reported by Ruiz-Moreno et al.[41]. They examined ChT using SS-OCT in 83 children (mean age 9.6 ± 3.1 years) with a mean refractive error of − 0.3 ± 2.0 D (range: −5.25 to 3.75 D) and reported a macular ChT of 285.2 ± 56.7 μm (range: 153–399 μm). These results closely align with our findings.

However, there are currently no published studies on ChT in the midperiphery of schoolchildren, except for our previous research involving adults. In that study, the ChT measurements in adults were 265.1 ± 85.0 μm in the macular region, 184.7 ± 48.1 μm in the nasal region, and 122.4 ± 31.6 μm in the temporal region[40]. A comparison of these results is presented in Fig. 5. While no significant differences in ChT were observed between schoolchildren and adults in the macular and nasal regions, the temporal region showed significantly thinner ChT in adults. It is important to note that the refractive error differed between the two groups. The adult group had a mean SE of − 4.11 ± 3.01 D, indicating a higher degree of myopia compared to the schoolchildren (mean SE: −1.25 ± 1.84 D). These findings suggest that with aging and the progression of myopia, ChT in the macular and nasal regions remains relatively stable,

while the temporal region becomes notably thinner. In other words, developmental changes in ChT in myopic eyes may be asymmetrical between the nasal and temporal regions. Further research is needed to investigate whether this asymmetry in ChT is related to asymmetric development of the eyeball, including changes in the sclera.

Significant correlations between ChT and both AL and SE were observed in the macular and temporal regions, but not in the nasal region. Subfoveal ChT has consistently been reported to significantly correlate with AL and SE[42–51], which aligns with our findings in the macular region. Interestingly, a significant correlation between ChT and both AL and SE was detected in the temporal midperiphery, whereas no such correlation was observed in the nasal midperiphery. This may suggest an asymmetrical elongation of the eyeball during myopia progression. Greater stretching on the temporal side could potentially drag retinal vessels toward the temporal periphery, contributing to increased optic disc tilting. These changes align with common features observed in color fundus photographs of myopic eyes, such as straightened temporal retinal vessels and pronounced optic disc tilting[52–54].

A key strength of this study is the use of 400 kHz SS-OCT, which enables high-speed imaging and reduces the effects of eye blinking and motion. The line scan pattern, completed in under 0.1 seconds with ample lateral sampling points and repetitions, provides clear, detailed images even in peripheral regions, facilitating precise choroidal analysis. However, this study also has limitations. As a cross-sectional study, it cannot establish a causal relationship between ChT, axial elongation, or myopia progression. Further longitudinal research, including analyses of ocular shape[55], is necessary to determine whether asymmetric thinning of peripheral ChT could serve as a predictor for myopia progression.

In conclusion, we quantitatively evaluated midperipheral ChT in schoolchildren and identified an asymmetrical pattern, with the macular region being the thickest, followed by the nasal region, and the temporal region being the thinnest. Significant correlations between ChT and both AL and SE were observed in the macular and temporal regions, whereas no such associations were found in the nasal region. When compared to adults, significant differences in ChT were observed only in the temporal region, where adults showed marked thinning. These findings suggest that choroidal thinning, particularly in the temporal region, may be primarily driven by ocular growth and the progression of myopia.

Methods

Participants

This prospective, observational, cross-sectional study was approved by the Institutional Review Board of the Riverside Clinic (Approval Number: RSC-2208RB02) and conducted at the Yoshino Eye Clinic. The study exclusively included healthy volunteers. Participants were children aged 6 to 18 years, while

exclusion criteria included individuals unable to provide consent, those with corneal, lens, or vitreous opacities that interfered with measurements, and cases deemed unsuitable by the examining physician.

Comprehensive ocular evaluations were performed, including slit-lamp examinations, AL measurements (MYAH; Topcon Corp., Tokyo, Japan), anterior segment OCT (CASIA2; Tomey Corp., Nagoya, Japan), and subjective refraction assessments. Additionally, widefield OCT imaging was conducted under cycloplegia induced by two applications of 1% cyclopentolate hydrochloride (Cyplegin® 1% ophthalmic solution; Santen Pharmaceutical Co., Ltd., Osaka, Japan) administered at 10-minute intervals. All measurements were performed between 10:00 AM and 5:00 PM. The study adhered to the principles outlined in the Declaration of Helsinki. Written informed consent was obtained from the parents or legal guardians of all participants, and written assent was obtained from the children after the study procedures were explained.

OCT Image Acquisition

In this study, we utilized a high-speed, wide-field SS-OCT prototype system (Topcon Corp., Tokyo, Japan). The specifications of this system have been described in previous reports, and the repeatability of its measurements has been validated[40]. In short, the system operates with a wavelength-tunable laser scanning at 400,000 A-scans per second within the 1-μm wavelength range, providing lateral and axial resolutions of approximately 18 μm and 9 μm (full-width at half-maximum) in tissue, respectively. The imaging depth range within tissue is 5.3 mm. A horizontal line scan pattern (15 mm, 1024 A-lines × 32 repeated B-scans) was employed in this study, with an acquisition time of less than 0.1 seconds. Measurements were performed using internal fixation for three regions: the macular area, 33° nasal, and 33° temporal from the fovea, respectively (Fig. 1). A total of three scans were completed within five minutes for each participant.

Choroidal Thickness (ChT) Measurements

Figure 2 shows the schematic of the ChT measurement, where three OCT images were distortion-corrected and converted to physical dimensions. Our definition of angle is the visual angle at the cornea. Bruch's membrane (BM) and the choroid-sclera interface (CSI) in each OCT image were automatically segmented, with manual corrections applied as needed to address segmentation errors. Three OCT images were corrected for distortion using a previously described method[56], resulting in actual-size representations of the images. By connecting the overlapping regions between the corrected images, the imaging range was extended to the vicinity of the equatorial region, as shown in Fig. 2(a). The average ChT value was calculated for a 3-mm region centered at a visual angle of 0° and at 39° on both the nasal and temporal sides. ChT was defined as the perpendicular distance from the BM line to the CSI line and was measured automatically using custom-designed software. The 3-mm range corresponded to the area extending 1.5 mm along the BM line from the central analysis point. Panels (b), (c), and (d) provide

magnified views of the area enclosed by the rectangle in Fig. 2 (a). The number of measurement points varied based on the distortion correction results, ranging from 164 to 281 points per scan.

Statistical analysis

Statistical analyses were performed using IBM SPSS Statistics version 26 (IBM Corp.). ChT across the three regions was compared using a one-way ANOVA with Bonferroni correction for multiple comparisons. The relationships between ChT and AL or spherical equivalent refractive error (SE) were assessed using Pearson's correlation test. Additionally, differences in ChT between schoolchildren and adults were evaluated using an unpaired t-test. A P-value of < 0.05 was considered statistically significant.

Abbreviations

OCT, optical coherence tomography; SS-OCT, swept-source optical coherence tomography; AL, axial length; SE, spherical equivalent refractive error; ChT, choroidal thickness; BM, Bruch’s membrane; CSI, choroid-sclera interface

Declarations

Acknowledgement

This work was supported in part by JSPS KAKENHI Grant Number 20K09783. The funders had no role in study design, data collection and analysis, decision to publish, or preparation of the manuscript.

Data availability statement

All data generated or analyzed during this study are included in this published article and its Supplementary Information files.

Financial Support: This work was supported by the JSPS KAKENHI Grant Number 20K09783.

Conflict of Interest: Tetsuro Oshikareceived research support from Topcon Corp. M.T., Y.M., R.K., T.M., and M.A. are employees of Topcon Corp. A.S. and K.S. are employees of Menicon Co., Ltd.

Author Contribution

T.H. and Y.M. designed the study. T.H., M.T., Y.M., and T.M. prepared the manuscript. M.A., Y.M., R.K., and T.M. prepared the device, and Y.T., K.Y., A.S., and K.S. collected the clinical data. M.A., Y.S., K.Y. and T.O. supervised the research. All authors reviewed and agreed with the manuscript.

References

1. Holden, B. A. et al. Global Prevalence of Myopia and High Myopia and Temporal Trends from 2000 through 2050. *Ophthalmology* **123**, 1036–1042 (2016).
2. Flitcroft, D. I. The complex interactions of retinal, optical and environmental factors in myopia aetiology. *Prog Retin Eye Res.* **31**, 622–660 (2012).
3. Naidoo, K. S. et al. Potential Lost Productivity Resulting from the Global Burden of Myopia: Systematic Review, Meta-analysis, and Modeling. *Ophthalmology* **126**, 338–346 (2019).
4. Wolffsohn, J. S. et al. IMI - Myopia Control Reports Overview and Introduction. *Invest. Ophthalmol. Vis. Sci.* **60**, M1–19 (2019).
5. Chen, Z. et al. Effects of Orthokeratology on Choroidal Thickness and Axial Length. *Optom. Vis. Sci.* **93**, 1064–1071 (2016).
6. Jin, W. Q. et al. Short term effect of choroid thickness in the horizontal meridian detected by spectral domain optical coherence tomography in myopic children after orthokeratology. *Int. J. Ophthalmol.* **11**, 991–996 (2018).
7. Li, Z. et al. Choroidal thickness and axial length changes in myopic children treated with orthokeratology. *Cont. Lens Anterior Eye*. **40**, 417–423 (2017).
8. Li, Z. et al. Change in subfoveal choroidal thickness secondary to orthokeratology and its cessation: a predictor for the change in axial length. *Acta Ophthalmol.* **97**, e454–459 (2019).
9. Lee, J. H. et al. Choroidal Thickness Changes after Orthokeratology Lens Wearing in Young Adults with Myopia. *Ophthalmic Res.* **64**, 121–127 (2021).
10. Ye, L. et al. Effects of atropine treatment on choroidal thickness in myopic children. *Invest. Ophthalmol. Vis. Sci.* **61**, 15 (2020).
11. Yam, J. C. et al. The association of choroidal thickening by atropine with treatment effects for myopia: Two-year clinical trial of the Low-concentration Atropine for Myopia Progression (LAMP) study. *Am. J. Ophthalmol.* **237**, 130–138 (2022).
12. Hao, Q. & Zhao, Q. Changes in subfoveal choroidal thickness in myopic children with 0.01% atropine, orthokeratology, or their combination. *Int. Ophthalmol.* **41**, 2963–2971 (2021).
13. Chamberlain, P. et al. A 3-year Randomized Clinical Trial of MiSight Lenses for Myopia Control. *Optom. Vis. Sci.* **96**, 556–567 (2019).
14. Prieto-Garrido, F. L. et al. Changes in the Choroidal Thickness of Children Wearing MiSight to Control Myopia. *J. Clin. Med.* **11**, 3833 (2022).
15. Breher, K. et al. The effect of the optical design of multifocal contact lenses on choroidal thickness. *PLoS One*. **13**, e0207637 (2018).
16. Lam, C. S. Y. et al. Defocus Incorporated Multiple Segments (DIMS) spectacle lenses slow myopia progression: a 2-year randomised clinical trial. *Br. J. Ophthalmol.* **104**, 363–368 (2020).
17. Chun, R. K. M. et al. Defocus incorporated multiple segments (DIMS) spectacle lenses increase the choroidal thickness: a two-year randomized clinical trial. *Eye Vis. (Lond)*. **10**, 39 (2023).

18. Jiang, Y. et al. Effect of Repeated Low-Level Red-Light Therapy for Myopia Control in Children: A Multicenter Randomized Controlled Trial. *Ophthalmology* **129**, 509–519 (2022).
19. Liu, G. et al. Axial Length Shortening and Choroid Thickening in Myopic Adults Treated with Repeated Low-Level Red Light. *J. Clin. Med.* **11**, 7498 (2022).
20. Zhao, C., Ni, Y. & Zeng, J. Effect of red-light therapy on retinal and choroidal blood perfusion in myopic children. *Ophthalmic Physiol. Opt.* **43**, 1427–1437 (2023).
21. Xiong, R. et al. Longitudinal Changes and Predictive Value of Choroidal Thickness for Myopia Control after Repeated Low-Level Red-Light Therapy. *Ophthalmology* **130**, 286–296 (2023).
22. Chen, H. et al. Low-intensity red-light therapy in slowing myopic progression and the rebound effect after its cessation in Chinese children: a randomized controlled trial. *Graefes Arch. Clin. Exp. Ophthalmol.* **261**, 575–584 (2023).
23. Wallman, J. et al. Moving the retina: Choroidal modulation of refractive state. *Vis. Res.* **35**, 37–50 (1995).
24. Wildsoet, C. & Wallman, J. Choroidal and scleral mechanisms of compensation for spectacle lenses in chicks. *Vis. Res.* **35**, 1175–1194 (1995).
25. Read, S. A., Collins, M. J. & Sander, B. P. Human optical axial length and defocus. *Invest. Ophthalmol. Vis. Sci.* **51**, 6262–6269 (2010).
26. Chakraborty, R., Read, S. A. & Collins, M. J. Monocular myopic defocus and daily changes in axial length and choroidal thickness of human eyes. *Exp. Eye Res.* **103**, 47–54 (2012).
27. Chakraborty, R., Read, S. A. & Collins, M. J. Hyperopic defocus and diurnal changes in human choroid and axial length. *Optom. Vis. Sci.* **90**, 1187–1198 (2013).
28. Drexler, W. et al. Eye elongation during accommodation in humans: differences between emmetropes and myopes. *Invest. Ophthalmol. Vis. Sci.* **39**, 2140–2147 (1998).
29. Shum, P. J. T. et al. A biometric study of ocular changes during accommodation. *Am. J. Ophthalmol.* **115**, 76–81 (1993).
30. Norton, T. T. Animal models of myopia: learning how vision controls the size of the eye. *ILAR J.* **40**, 59–77 (1999).
31. Wildsoet, C. F. Active emmetropization–evidence for its existence and ramifications for clinical practice. *Ophthalmic Physiol. Opt.* **17**, 279–290 (1997).
32. Summers, J. A. The choroid as a sclera growth regulator. *Exp. Eye Res.* **114**, 120–127 (2013).
33. Troilo, D., Nickla, D. L. & Wildsoet, C. F. Choroidal thickness changes during altered eye growth and refractive state in a primate. *Invest. Ophthalmol. Vis. Sci.* **41**, 1249–1258 (2000).
34. Verkicharla, P. K. et al. Eye shape and retinal shape, and their relation to peripheral refraction. *Ophthalmic Physiol. Opt.* **32**, 184–199 (2012).
35. Gentle, A. et al. Collagen gene expression and the altered accumulation of scleral collagen during the development of high myopia. *J. Biol. Chem.* **278**, 16587–16594 (2003).

36. Tanihara, H. et al. Clinical features of retinal detachment in the elderly. *Ophthalmologica* **209**, 203–207 (1995).
37. Hirano, M. et al. Analysis of widefield choroidal thickness maps of healthy eyes using swept source optical coherence tomography. *Sci. Rep.* **13**, 11904 (2023).
38. Liu, X. et al. New findings on choroidal features in healthy people by ultra-widefield swept-source optical coherence tomography angiography. *Sci. Rep.* **13**, 9215 (2023).
39. Funatsu, R. et al. NORMAL PERIPHERAL CHOROIDAL THICKNESS MEASURED BY WIDEFIELD OPTICAL COHERENCE TOMOGRAPHY. *Retina* **43**, 490–497 (2023).
40. Hiraoka, T. et al. Choroidal thickness in macular, nasal midperiphery, and temporal midperiphery regions and its relationship with axial length and refractive error. *Jpn J. Ophthalmol.* **69**, 24–31 (2025).
41. Ruiz-Moreno, J. M. et al. Macular choroidal thickness in normal pediatric population measured by swept-source optical coherence tomography. *Invest. Ophthalmol. Vis. Sci.* **54**, 353–359 (2013).
42. Ouyang, Y. et al. Spatial distribution of posterior pole choroidal thickness by spectral domain optical coherence tomography. *Invest. Ophthalmol. Vis. Sci.* **52**, 7019–7026 (). (2011).
43. Li, X. Q., Larsen, M. & Munch, I. C. Subfoveal choroidal thickness in relation to sex and axial length in 93 Danish university students. *Invest. Ophthalmol. Vis. Sci.* **52**, 8438–8441 (2011).
44. Esmaeelpour, M. et al. Three-dimensional 1060-nm OCT: choroidal thickness maps in normal subjects and improved posterior segment visualization in cataract patients. *Invest. Ophthalmol. Vis. Sci.* **51**, 5260–5266 (2010).
45. Wei, W. B. et al. Subfoveal choroidal thickness: the Beijing Eye Study. *Ophthalmology* **120**, 175–180 (2013).
46. Tan, C. S. & Cheong, K. X. Macular choroidal thicknesses in healthy adults–relationship with ocular and demographic factors. *Invest. Ophthalmol. Vis. Sci.* **55**, 6452–6458 (2014).
47. Chen, F. K. et al. Topographic variation and interocular symmetry of macular choroidal thickness using enhanced depth imaging optical coherence tomography. *Invest. Ophthalmol. Vis. Sci.* **53**, 975–985 (2012).
48. Vincent, S. J. et al. Retinal and choroidal thickness in myopic anisometropia. *Invest. Ophthalmol. Vis. Sci.* **54**, 2445–2456 (2013).
49. Li, X. Q. et al. Choroidal thickness in relation to birth parameters in 11- to 12-year-old children: the Copenhagen Child Cohort 2000 Eye Study. *Invest. Ophthalmol. Vis. Sci.* **56**, 617–624 (2014).
50. Zhang, J. M. et al. Macular choroidal thickness in children: the Shandong Children Eye Study. *Invest. Ophthalmol. Vis. Sci.* **56**, 7646–7652 (2015).
51. Deng, J. et al. Distribution pattern of choroidal thickness at the posterior pole in Chinese children with myopia. *Invest. Ophthalmol. Vis. Sci.* **59**, 1577–1586 (2018).
52. Jonas, R. A. et al. Elongation of the disc-fovea distance and retinal vessel straightening in high myopia in a 10-year follow-up of the Beijing eye study. *Sci. Rep.* **11**, 9006 (2021).

53. Jonas, J. B. et al. Myopia: Histology, clinical features, and potential implications for the etiology of axial elongation. *Prog Retin Eye Res.* **96**, 101156 (2023).
54. Mi, X. et al. Temporal vascular arcade angle in fundus image was associated with the rate of spherical equivalent refractive error and axial length changes in myopia children with young school age. *Photodiagnosis Photodyn Ther.* **49**, 104305 (2024).
55. Hiraoka, T. et al. Quantitative Mapping of Posterior Eye Curvature in Children Using Distortion-Corrected OCT: Insights into temporal region morphology. *Ophthalmol. Sci.* **5**, 100695 (2025).
56. Izumi, T. et al. Morphological differences of choroid in central serous chorioretinopathy determined by ultra-widefield optical coherence tomography. *Graefes Arch. Clin. Exp. Ophthalmol.* **260**, 295–301 (2022).

Figures

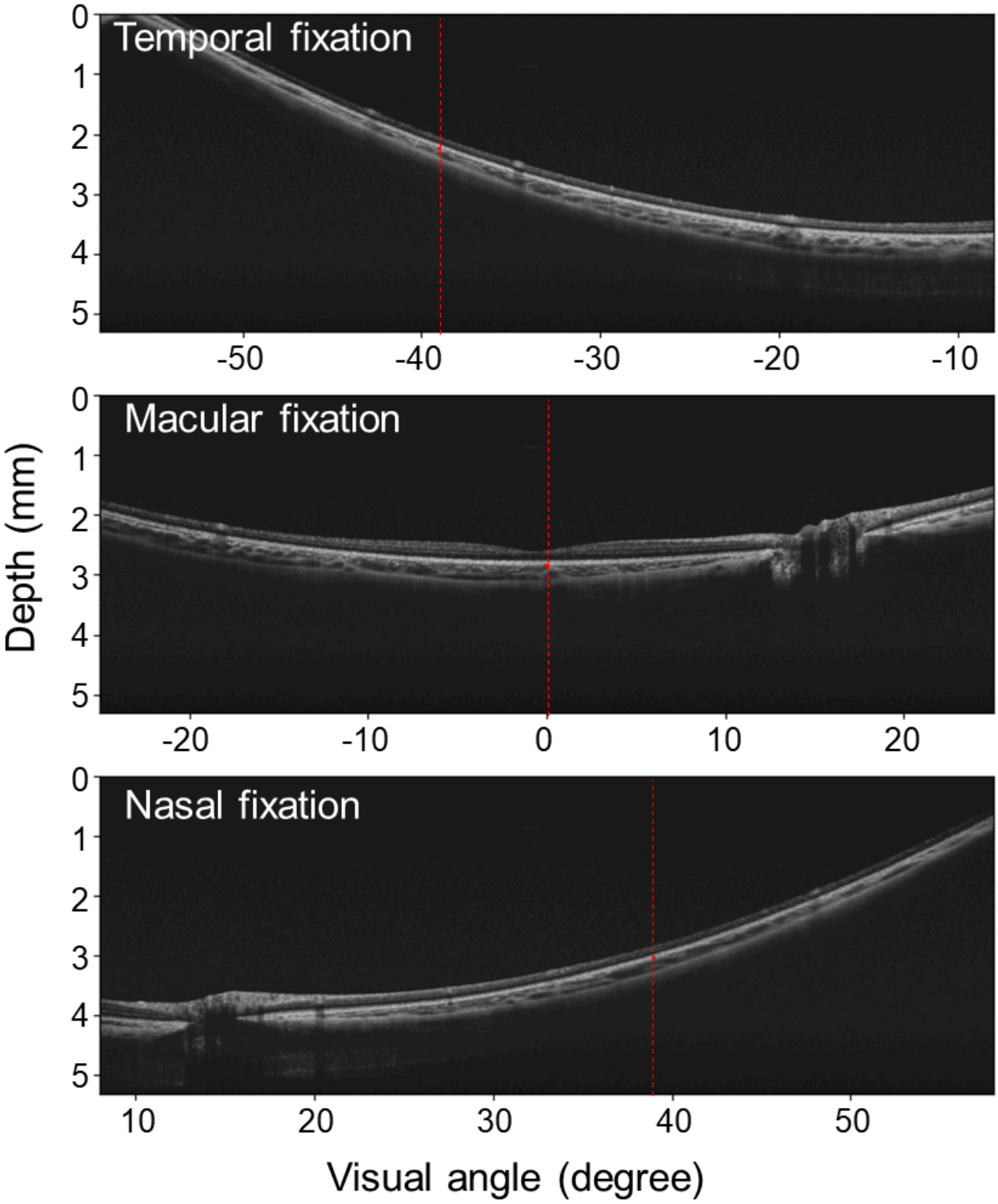


Figure 1

Three line-scans performed on each subject in this study.

Choroidal thickness (ChT) was measured in three regions centered on nasal 39 degrees, 0 degrees, and temporal 39 degrees. The central angles of these regions are marked by red dashed lines.

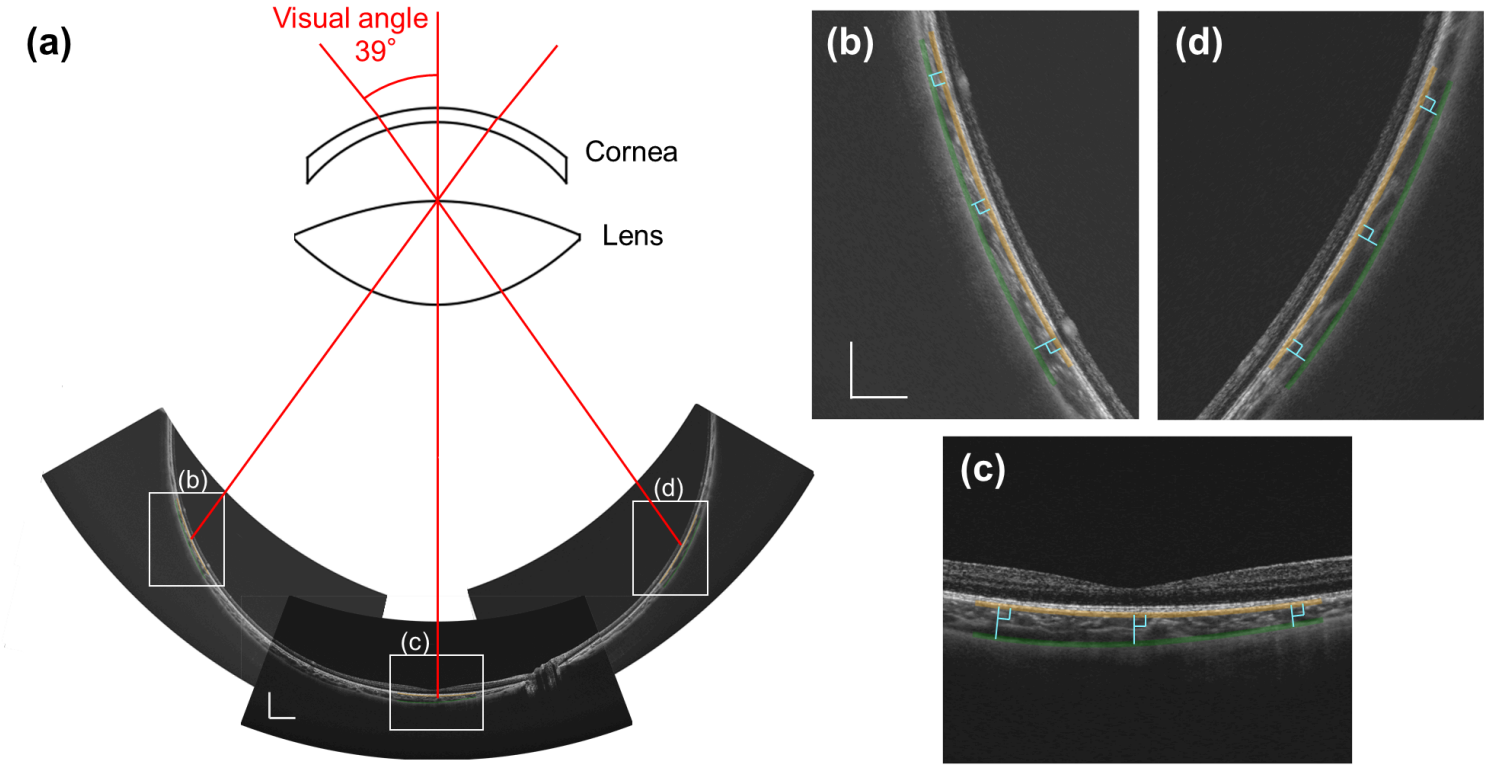


Figure 2

Schematic diagram of the choroidal thickness (ChT) measurements using optical coherence tomography (OCT).

(a) Distortion corrected montage OCT B-frame image with visual angle schematic. Scale bar: 1 mm. (b-d) Magnified views of the three regions of interest shown in (a). Orange lines indicate the segmented Bruch's membrane (BM) lines used for the analysis in 3 mm-length. ChT was measured perpendicularly as the distance from BM to the choroid-sclera interface CSI (green lines). Scale bar: 500 μm.

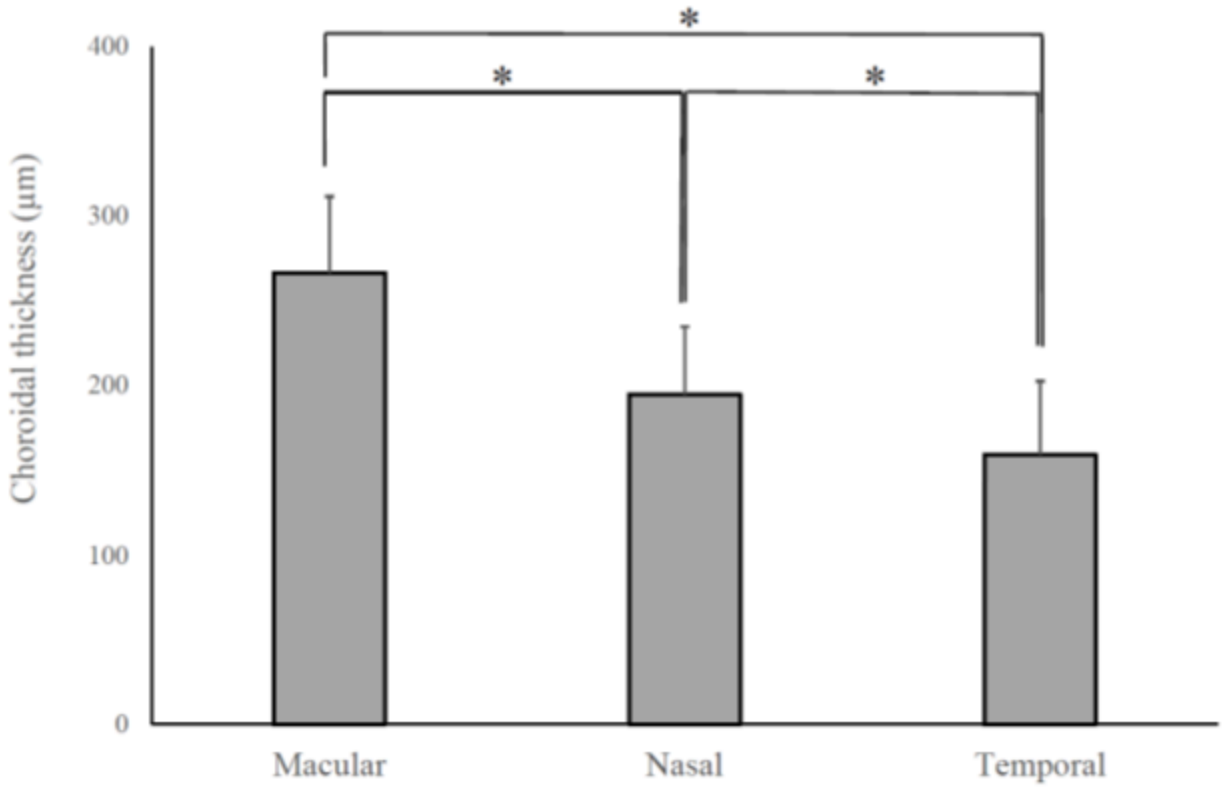


Figure 3

Comparison of choroidal thickness (ChT) between three regions.

The results of ChT for each region were as follows: 266.3 ± 63.2 μm in the macular region, 194.4 ± 39.5 μm in the nasal midperiphery region, and 158.7 ± 41.4 μm in the temporal midperiphery region. Significant differences were observed between the three regions ($P < 0.0001$, One-way ANOVA), with the macular region having the largest ChT, followed by the nasal midperiphery region, and then the temporal midperiphery region ($P < 0.0001$ for all combinations, Bonferroni correction).

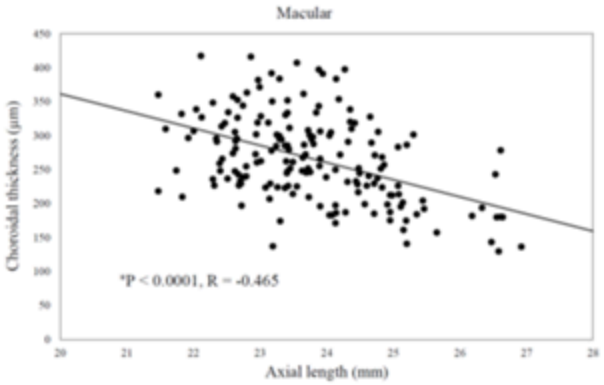


Figure 4a.

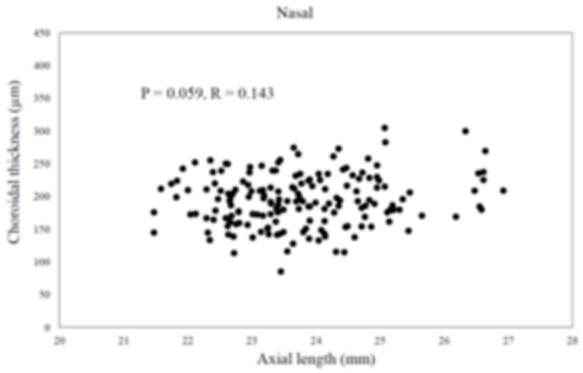


Figure 4b.

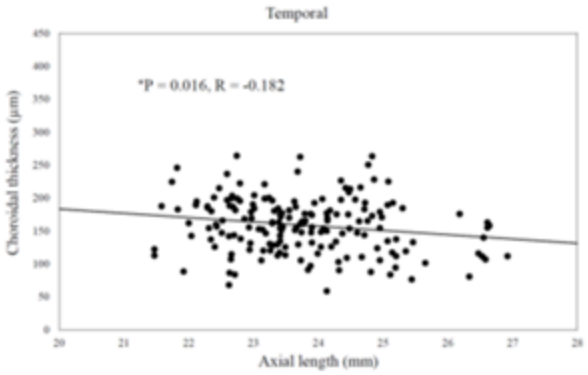


Figure 4c.

Figure 4

Scatter plots between ChT and AL.

(a) Macular region. (b) Nasal midperiphery region. (c) Temporal midperiphery region. Significant relationships were observed in the macular (P < 0.0001, R = −0.465, Pearson correlation test) and temporal midperiphery (P = 0.016, R = −0.182) regions, but not in the nasal midperiphery region (P = 0.059, R = 0.143).

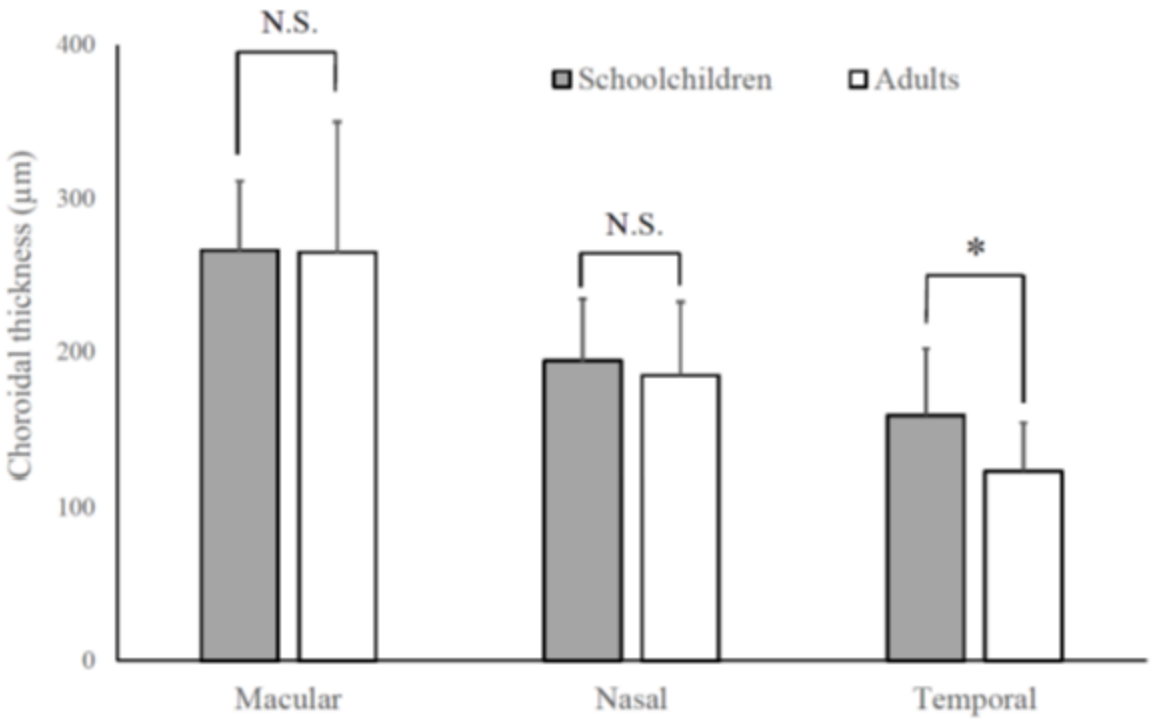


Figure 5

Comparison of ChT between schoolchildren and adults.

There were no significant differences between the schoolchildren and adults in the macular and nasal regions (P = 0.943 and 0.313, respectively, unpaired t-test), however, there was a significant difference between them in the temporal region (P < 0.0001).

Supplementary Files

This is a list of supplementary files associated with this preprint. Click to download.

- DataSet.xlsx